

Effects of simulated Secondary Organic Aerosol Water on ~~fine~~ PM₁ levels and composition over US

Stylianos Kakavas^{1,2}, Spyros N. Pandis^{1,2} and Athanasios Nenes^{1,3}

¹Institute of Chemical Engineering Sciences, Foundation for Research and Technology Hellas, Patras, Greece

²Department of Chemical Engineering, University of Patras, Patras, Greece

³School of Architecture, Civil and Environmental Engineering, École Polytechnique Fédérale de Lausanne (EPFL), Switzerland

Correspondence to: [Athanasios Nenes \(athanasios.nenes@epfl.ch\)](mailto:athanasios.nenes@epfl.ch) and [Spyros N. Pandis \(spyros@chemeng.upatras.gr\)](mailto:spyros@chemeng.upatras.gr).

~~[Spyros N. Pandis \(spyros@chemeng.upatras.gr\)](mailto:spyros@chemeng.upatras.gr) and [Athanasios Nenes \(athanasios.nenes@epfl.ch\)](mailto:athanasios.nenes@epfl.ch).~~

Abstract. Water is a key component of atmospheric aerosol, affecting many aerosol processes including gas/particle partitioning of semi-volatile compounds. Water related to secondary organic aerosol (SOAW) is often neglected in atmospheric chemical transport models and is not considered in gas-to-particle partitioning calculations for inorganic species. We use a new inorganic aerosol thermodynamics model, ISORROPIA-lite, which considers the effects of SOAW, to perform chemical transport model simulations for a year over the continental United States to quantify its effects on aerosol mass concentration and composition. SOAW can increase average fine aerosol water levels up to a factor of two when secondary organic aerosol (SOA) is a major PM₁ component. This is often the case in the south-eastern U.S where SOA concentrations are higher. Although the annual average impact of this added water on total dry PM₁ concentrations due to increased partitioning of nitrate and ammonium is small (up to 0.1 μg m⁻³), total dry PM₁ increases of up to 2 μg m⁻³ (with nitrate levels increases up to 200%) can occur when RH levels and PM₁ concentrations are high.

1. Introduction

Commented [Σ1]: Reviewer 4 Comment 4

Formatted: English (United States)

34 Atmospheric particulate matter with aerodynamic diameter smaller than 1 μm (PM_{10})
35 has adverse effects on public health, climate and ecosystem productivity (Pye et al.,
36 2020; Baker et al., 2021; Guo et al., 2021). PM_{10} is composed of thousands of organic
37 compounds, black carbon (BC), and inorganic components such as sulfate (SO_4^{2-}),
38 nitrate (NO_3^-), ammonium (NH_4^+) and chloride (Cl^-) (Seinfeld and Pandis, 2006).
39 Ambient aerosol is mostly composed of water which is determined by the chemical
40 equilibrium of water vapor with the aerosol constituents (Liao and Seinfeld, 2005;
41 Carlton and Turpin, 2013; Bian et al., 2014; Guo et al., 2015; Bougiatioti et al., 2016;
42 Nguyen et al., 2016; Guo et al., 2017; Deetz et al., 2018; Kuang et al., 2018; Song et
43 al., 2018; Wu et al., 2018; Pye et al., 2020; Gopinath et al., 2022). Aerosol liquid
44 water directly affects the PM sensitivity and dry deposition rates, with direct
45 implications for emissions control policy (Nenes et al., 2020; Nenes et al., 2021; Sun
46 et al., 2021).

47 The hygroscopicity parameter (κ), which expresses the ability of a PM
48 component to absorb water, is an effective approach for the parameterization of the
49 water uptake of atmospheric PM that is a mixture of organic and inorganic species
50 (Petters and Kreidenweis, 2007). Although organic aerosol (OA) is less hygroscopic
51 than inorganic salts, it can still contribute significantly to the total aerosol water (Guo
52 et al., 2015; Bougiatioti et al., 2016; Jathar et al., 2016; Li et al., 2019) or can even
53 become the dominant contributor at lower ambient relative humidity (Jin et al., 2020).
54 Previous studies have demonstrated that secondary organic aerosol (SOA) is a lot
55 more hygroscopic ($0.1 \leq \kappa \leq 0.3$) than primary organic aerosol (POA) ($\kappa \leq 0.01$) and
56 is mainly responsible for the corresponding OA water (Petters et al., 2006; Koehler et
57 al., 2009; Chang et al., 2010; Jathar et al., 2016; Kuang et al., 2020; Li et al., 2020).

58 SOAW can enhance secondary inorganic aerosol concentrations assisting in
59 their partitioning in the particulate phase to satisfy equilibrium. However, such effects
60 are not considered in thermodynamic modules used for the simulation of gas-to-
61 particle partitioning of inorganic species in chemical transport models. Evidence
62 exists however that fine aerosol nitrate and ammonium concentrations can increase in
63 areas with high organic aerosol and RH levels (Kakavas et al., 2022). The importance
64 of these SOAW impacts on secondary aerosol formations has not been systematically
65 studied and is the focus of this work.

66 We use a new aerosol thermodynamics model, ISORROPIA-lite (Kakavas et
67 al., 2022), to simulate SOAW effects on the partitioning of the inorganic components,

68 for a year over the continental United States. The model performance has been
69 evaluated for fine PM and its components for the examined period by Skyllakou et al.
70 (2021). It is considered good for the total PM_{2.5} concentration and average for most of
71 the components. The aim of our work is to quantify the SOAW contribution to the
72 total fine PM water and to study its effects on inorganic aerosol thermodynamics and
73 total dry fine PM levels and composition.

74

75 2. Methods

76 2.1 ISORROPIA-lite

77 ISORROPIA-lite is a lean and accelerated version of the widely used ISORROPIA-II
78 (Fountoukis and Nenes, 2007) aerosol thermodynamics model and it focuses on the
79 simulation of the composition of the inorganic fraction of the atmospheric aerosol that
80 is in equilibrium with the gas phase. ~~and it focuses on the simulation of the~~
81 ~~thermodynamic equilibrium of inorganic atmospheric aerosol.~~ It assumes that the
82 aerosol exists only in the metastable state at low RH and the activity coefficients of
83 ionic pairs are always obtained from precalculated look-up tables. It estimates aerosol
84 water associated with each one of the aerosol components. Furthermore,
85 ISORROPIA-lite has an important additional feature compared to ISORROPIA-II, as
86 it considers the effects of SOAW on inorganic aerosol thermodynamics. The resulting
87 increase of the total water mass drives more of the water-soluble gaseous species to
88 the particle phase to satisfy equilibrium. SOAW, W_{SOA} , in ISORROPIA-lite is
89 calculated using the well-established κ -Kohler theory of Petters and Kreidenweis
90 (2007):

91

$$W_{SOA} = \frac{\rho_w}{\rho_{SOA}} \frac{C_{SOA} \kappa}{\left(\frac{1}{RH} - 1\right)} \quad (1)$$

92 where ρ_w is the density of water, ρ_{SOA} the SOA density, C_{SOA} the SOA concentration, κ
93 the SOA hygroscopicity parameter and RH the relative humidity in the 0–1 scale.
94 More details about the ISORROPIA-lite can be found in Kakavas et al. (2022).

95

96 2.2 PMCAMx description and application

97 PMCAMx (Karydis et al., 2010; Tsimpidi et al., 2010) is a three dimensional
98 chemical transport model based on CAMx (Environ, 2006), which simulates
99 horizontal and vertical advection and dispersion, dry and wet deposition, as well as

Commented [Σ2]: Reviewer 3 Comment 2
Reviewer 4 Comment 2

Commented [Σ3]: Reviewer 3 Comment 2
Reviewer 4 Comment 2

100 aqueous, gas, and aerosol chemistry. The mechanism used in this work for gas-phase
101 chemistry simulations is the Carbon Bond 05 (CB5) (Yarwood et al., 2005) and
102 includes 190 reactions of 79 gas species. To describe the aerosol size and composition
103 distribution 10-size sections (from 40 nm to 40 μm) are used assuming that all
104 particles in each size bin have the same composition. Therefore, PMCAMx predicts
105 PM_x concentrations where x can be among other choices 1, 2.5 and 10 μm .
106 Equilibrium is always assumed between the bulk aerosol and gas phases. The
107 partitioning of semi-volatile inorganic species between the gas and particulate phases
108 is simulated by ISORROPIA-lite. Weighting factors based on the effective surface
109 area of each size bin are ~~Weighting factors based on each size bin's effective surface~~
110 ~~area are~~ used to distribute to the various size bins the mass transferred between the
111 two phases in each time step (Pandis et al., 1993). For the simulation of organic
112 aerosols, the volatility basis set (VBS) approach (Donahue et al., 2006) is used. POA
113 is simulated using eight volatility bins (from 10^{-1} to $10^6 \mu\text{g m}^{-3}$) at 298 K, while for
114 SOA four volatility bins (1, 10, 10^2 , $10^3 \mu\text{g m}^{-3}$) at 298 K are used (Murphy and
115 Pandis, 2009). An organic aerosol phase is assumed with its components forming a
116 pseudo-ideal solution and being in equilibrium with the ~~The gas phase and aerosol~~
117 ~~phases of the organic components are assumed to be in equilibrium~~ (Strader et al.,
118 1998). The influence of water on the partitioning of the organic components of the
119 particulate matter between the gas and aerosol phases is assumed to be negligible in
120 this version of PMCAMx as implemented by Koo et al. (2003). The partitioning
121 between the gas and aerosol phases is similar to the inorganics but includes an
122 additional factor to account for the aerosol composition using a pseudo ideal
123 assumption (Koo et al., 2003). The low volatility organic compounds (LVOCs) and
124 the extremely LVOCs are implicitly included in the lowest volatility bin of this
125 version of the VBS used in PMCAMx. These compounds are always in the particulate
126 phase in these simulations and therefore the addition of lower bins increases the
127 computational cost without changing the predicted organic aerosol concentration. For
128 the major point sources, the NO_x plumes are simulated using the Plume-in-Grid (PiG)
129 approach (Karamchandani et al., 2011; Zakoura and Pandis, 2019). For the simulation
130 of aqueous-phase chemistry, ~~The~~ variable size resolution model (VSRM) of Fahey
131 and Pandis (2001) is used for the simulation of aqueous-phase. The model is based on
132 the chemical mechanism of Pandis and Seinfeld (1989) with the addition of Ca^{2+} to

Commented [S4]: Reviewer 4 Comment 2

Commented [S5]: Reviewer 4 Comment 6

133 the list of particle components as well as H₂SO₄ in the gas phase (Fahey and Pandis,
134 2001).

Commented [Σ6]: Reviewer 3 Comment 2

135 We applied PMCAMx over the continental United States during 2010. The
136 modeling domain includes northern Mexico and southern Canada and covers a 4752 ×
137 2952 km² region (Figure S1). The model grid consists of 10,824 cells with horizontal
138 dimensions of 36 × 36 km. The meteorological inputs were provided by the Weather
139 Research Forecasting model (WRF v3.6.1) using a horizontal resolution of 12 ×
140 12 km. ~~Therefore, RH levels above 95% were not predicted that frequently rare~~
141 ~~therefore there was no need for screening of the few high RH values outside clouds.~~
142 ~~do not suffer from the corresponding experimental challenges and there was no need~~
143 ~~for screening of the few values above 95%.~~ The gaseous and primary particle
144 emissions were developed by Xing et al. (2013). More details about the
145 meteorological inputs and the emissions can be found in Skyllakou et al. (2021).

Commented [Σ7]: Reviewer 4 Comment 7

146 To quantify the SOAW effects on inorganic aerosol thermodynamics three
147 simulations were performed. The first was a simulation neglecting SOAW and
148 including only inorganic aerosol water. ~~Two additional simulations were performed:~~
149 ~~one where κ of SOA was assumed to be equal to 0.1 and one with κ=0.2 (Kuang et al.,~~
150 ~~2020) to examine how SOA hygroscopicity affects total fine aerosol water content~~
151 ~~and PM levels and composition. Even if higher values of the hygroscopicity~~
152 ~~parameter (e.g., κ=0.3) are possible (Kuang et al., 2020) these represents rather~~
153 ~~an extreme cases for the simulation of the average effects over the US. Therefore, the~~
154 ~~two simulations used in this study provide a good estimate of the corresponding~~
155 ~~uncertainty.~~ Previous studies have estimated secondary organic aerosol density values
156 of 1–1.4 g cm⁻³ (Turpin and Lim, 2001; ~~Konstenidou~~Kostenidou et al., 2007). A SOA
157 density of 1 g cm⁻³ was assumed in the simulations ~~because higher densities suggest~~
158 ~~that SOA particles may be in solid or waxy state (Konstenidou et al., 2007).~~ The SOA
159 exists mostly in submicrometer particles so our subsequent study focuses on PM₁.

Commented [Σ8]: Reviewer 4 Comment 8

Commented [ΣP9]: Reviewer 4, Comment 5

161 3. Results

162 3.1 Effects of SOAW on PM₁ water levels

163 The annual average PM₁ water ground-level concentrations neglecting SOAW are
164 shown in Figure 1. Higher PM₁ water concentrations from 8 to 18 μg m⁻³ are
165 predicted in the north-eastern part of the US due to the higher inorganic PM₁
166 concentrations (Figure 2) and RH levels in that area. When SOAW is present in the

167 simulations, total PM₁ water levels increase everywhere with higher fractional
168 increases in the south-eastern US (up to 50% when $\kappa=0.1$ and up to 100% when $\kappa=0.2$
169 in Alabama and north-western Mexico) due to higher SOA levels (Figure S2). In the
170 north-eastern US, lower fractional increases are predicted (10–15% when $\kappa=0.1$ and
171 20–30% when $\kappa=0.2$). In general, assuming a κ of SOA equal to 0.2 instead of 0.1
172 increases the corresponding amount of SOAW by about a factor of two. Figure 1
173 shows the distributions of fractional increase change in the annual PM₁ water levels at
174 ground level from SOAW. Total PM₁ water average concentrations increase from 20
175 to 30% in about 60% of the modeling domain when $\kappa=0.1$. For $\kappa=0.2$, the
176 corresponding increase is from 40 to 60%.

177 Predicted SOA levels are higher during summertime (Figure S2) since the
178 emissions and oxidation rates of volatile organic compounds (VOCs) are higher
179 (Zhang et al., 2013; Freney et al., 2014; Skyllakou et al., 2014; Fountoukis et al.,
180 2016). However, even during wintertime fresh biomass burning emissions exposed to
181 NO₂ and O₃ can form significant amounts of SOA in periods with low OH levels
182 (Kodros et al., 2020). Higher total PM₁ water concentrations are predicted during
183 winter (Figure 3) since the RH levels and inorganic fine aerosol concentrations are
184 higher; especially nitrate and chloride which increasingly partition to the aerosol
185 phase as temperature decreases (Guo et al., 2017). However, PM₁ chloride
186 concentrations are low (less than 0.1 $\mu\text{g m}^{-3}$) with higher concentrations in Kansas
187 because of biomass burning episodes. Higher fractional increases in fine aerosol water
188 levels (up to 5 times) due to SOAW are predicted during summer in the south-eastern
189 part of US where SOA concentrations are higher. This corresponds to increases to
190 average fine aerosol water concentrations up to 8 $\mu\text{g m}^{-3}$.

191 Ammonium nitrate and ammonium sulfate are the inorganic salts that
192 contribute the most to the total PM₁ water levels (Figure S3). SOAW also contributes
193 significantly to the total PM₁ water levels especially in the south-eastern US (about 30
194 and 50% of total PM₁ water when $\kappa=0.1$ and $\kappa=0.2$ respectively), when the mass
195 fraction of SOA in dry PM₁ exceeds 30%.

196

197 **3.2 Effects of SOAW on total dry PM₁ levels**

198 Higher dry PM₁ concentrations are predicted for the eastern part of the US (up to 15
199 $\mu\text{g m}^{-3}$) in the base case (Figure 4). These dry PM₁ levels increase slightly up to 0.6%
200 and 1.2% due to SOAW when $\kappa=0.1$ and $\kappa=0.2$ for SOA is assumed. The highest

201 annual average fractional increase in total dry PM_1 levels is predicted in California
202 (1% when $\kappa=0.1$ and 2% when $\kappa=0.2$). The probability density (Figure 4) indicates
203 that in about 60% of the modeling domain total dry fine aerosol concentrations
204 increase up to 0.3% when $\kappa=0.1$. For $\kappa=0.2$, the corresponding increase is from 0.4 to
205 2%. The areas of the highest PM_1 increase correspond to regions where aerosol pH
206 tends to be relatively high (Pye et al., 2020). In these areas, nitric acid and ammonia
207 can condense and increase aerosol mass because of the increase in water from the
208 SOA. Because of this partitioning change, the predicted gas-phase concentrations of
209 semi-volatile inorganic components decreased on average when SOAW was
210 considered (Figure S4). SOAW had a negligible absolute impact on the small fine
211 chloride concentrations in this period (Figure 2). However, in periods during which
212 chloride salts and SOA contribute significantly to the total dry (e.g. during intense
213 biomass burning periods), fine chloride concentrations could also change (Metzger et
214 al., 2006; Fountoukis et al., 2009; Gunthe et al., 2021).

215 Skyllakou et al. (2021) found that PMCAMx had a small fractional bias (5%)
216 and a fractional error (25%) for the annual average $PM_{2.5}$ concentrations of 1067
217 measurements stations in the U.S. The performance of PMCAMx regarding annual
218 average OA is considered good in these simulations with a fractional bias of 5% and a
219 fractional error of 26% in the 306 stations in the US. For daily average concentrations
220 the performance is also quite encouraging with a fractional bias of 15% and a
221 fractional error of 56%. Given that the effect of the extension of the model on the total
222 fine PM mass is small (of the order of 1%), this does not result in any noticeable
223 change in its already very good performance for dry fine PM. Therefore, the major
224 change in the model predictions is on the aerosol water concentrations.

225

226 3.3 Effects of SOAW on PM_1 components

227 The annual average results indicate that SOAW mainly affects fine aerosol water
228 levels. To better analyze the effects of SOAW we focus on the temporal evolution of
229 the predicted levels of PM_1 components in four sites (Figure S1) with different
230 characteristics (Table S1). We have chosen one city from the West, one from the
231 South, one from Southeast and one from the Northeast. They are all in different
232 environments with different major sources and climatological conditions. The
233 presence of SOAW increased PM_1 water concentrations in all sites from 1% to almost
234 an order of magnitude (Figure 5). However, these fractional increases most of the

235 time correspond to PM₁ water concentration increases of a few $\mu\text{g m}^{-3}$ (Figure S56)
236 because they occur under low RH levels. During higher RH periods (80 to 100%), the
237 PM₁ water levels are predicted to increase up to $100 \mu\text{g m}^{-3}$ (e.g. in Toronto).

238 Total dry PM₁ concentrations during most of the simulated period increase on
239 average less than 1% in all sites (Figure 5) due to SOAW. There are periods, however,
240 with higher fractional increases (up to 10%) and even small decreases (up to 5%) in
241 total dry fine aerosol levels in the examined sites. The decreases can be explained
242 because SOAW increases the size of particles and therefore their dry deposition rate
243 (Nenes et al., 2020). Depending on SOA hygroscopicity, increases up to $1.5 \mu\text{g m}^{-3}$
244 for nitrate and $0.5 \mu\text{g m}^{-3}$ for ammonium are predicted (Figure S56). Fine nitrate
245 increases of 10% were more frequent in the examined sites; however higher increases
246 up to 200% are predicted during the simulated period (Figure 67). As expected, higher
247 increases can occur more often with higher assumed SOA hygroscopicity.

248

249 4. Discussion

250 Aerosol liquid water has a profound impact on aerosol processes, chemical
251 composition and their impacts. By including the effects of organic water on
252 inorganics thermodynamic equilibrium we show that SOAW can substantially
253 increase aerosol water levels, on an average up to 60% over the majority of the
254 domain. As a consequence, total dry PM₁ levels can also increase but the changes are
255 small (up to 2% on an annual average basis). Locally these effects can be much more
256 significant during periods of high RH and SOA levels (fine nitrate fractional increases
257 can be as high as 200%).

258 The effects vary with season. During summer, the RH is lower and SOA levels
259 are higher leading to higher fractional increases in aerosol water (Figure 3) but lower
260 absolute mass changes. During summer the fractional increases in total dry fine
261 aerosol concentrations are lower than in wintertime (Figure S65). Responsible for the
262 total dry fine aerosol concentration increases are nitrate and ammonium (Figure 2).
263 These compounds partition together (as deliquesced ammonium nitrate) to the
264 particulate phase to satisfy equilibrium due to the additional water mass of SOA.

265 The increases in total dry PM₁ and fine aerosol water levels depend on SOA
266 concentrations, hygroscopicity value, RH levels and the particle phase fractions of
267 inorganic species. The SOAW effect on aerosol water is approximately proportional
268 to the assumed hygroscopicity parameter κ . Given that our work investigates the

269 potential significance of this effect we have chosen to provide the results of two
270 simulations one with relatively low and relatively high hygroscopicity of SOA. A
271 more detailed treatment of the hygroscopicity parameter (e.g., assigning a different
272 value to each OA component) will be a topic of future work.

273 The present work, thoroughly analyzes organic water uptake impacts over one
274 simulated year (not just one month as done in Kakavas et al., 2022) and in quite a
275 different geographical area (US here versus Europe in Kakavas et al., 2022). There are
276 significant differences, but also similarities in the predicted changes and effects of
277 SOA water. Both studies indicate that SOAW can contribute highly to the total PM₁
278 water and increase particulate nitrate concentrations especially in areas with high total
279 nitrate concentrations. Pilinis et al. (1995) have argued that the single most important
280 parameter in determining direct aerosol forcing is RH, and the most important process
281 is the increase of the aerosol mass as a result of water uptake. They estimated that on
282 average an increase of the RH from 40 to 80% for a global mean aerosol more than
283 doubles the corresponding radiative forcing. As a result the inclusion ~~It is expected~~
284 the direct radiative forcing due to more scattering caused by increased aerosol water
285 to be increased up to an order of magnitude (Pilinis et al., 1995). Given this, and the
286 important role of SOAW for climate forcing, visibility and chemistry, its inclusion in
287 future studies is highly recommended. ISORROPIA-lite provides a simple and
288 computationally effective approach for the simulation of this SOAW.

289
290 **Code and Data Availability.** The model code and data used in this study are available
291 from the authors upon request (spyros@chemeng.upatras.gr and
292 athanasios.nenes@epfl.ch).

293
294 **Author Contributions.** SK incorporated ISORROPIA-lite in PMCAMx, carried out the
295 simulations, analyzed the results and wrote the manuscript. SN and AN conceived and
296 led the study and helped in the writing of the manuscript. [All authors contributed to the](#)
297 [reviewer responses and manuscript revisions.](#)

298
299 **Competing Interests.** The authors declare no competing financial interest.

300
301 **Acknowledgements.** This work was supported by the project FORCeS funded from
302 the European Union's Horizon 2020 research and innovation programme under grant

Formatted: English (United States)

Formatted: English (United States)

Formatted: English (United States)

Commented [SP10]: Reviewer 3, Comment 3

Formatted: English (United States)

Formatted: English (United States)

303 agreement No 821205, and project PyroTRACH (ERC-2016-COG) funded from
304 H2020-EU.1.1. - Excellent Science - European Research Council (ERC), project ID
305 726165.

306

307 **References**

308 Baker, A., Kanakidou, M., Nenes, A., Myriokefalitakis, S., Croot, P.L., Duce, A. D.,
309 Gao, Y., Guieu, C., Ito, A., Jickells, T. D., Mahowald, N. M., Middag, R.,
310 Perron, M. M. G., Sarin, M. M., Shelley, R., and Turner, D. R.: Changing
311 atmospheric acidity as a modulator of nutrient deposition and ocean
312 biogeochemistry, *Sci. Adv.*, 7, doi: 10.1126/sciadv.abd8800, 2021.

313 Bian, Y. X., Zhao, C. S., Ma, N., Chen, J., and Xu, W. Y.: A study of aerosol liquid
314 water content based on hygroscopicity measurements at high relative humidity
315 in the North China Plain, *Atmos. Chem. Phys.*, 14, 6417–6426, 2014.

316 Bougiatioti, A., Nikolaou, P., Stavroulas, I., Kouvarakis, G., Weber, R., Nenes, A.,
317 Kanakidou, M., and Mihalopoulos, N.: Particle water and pH in the eastern
318 Mediterranean: source variability and implications for nutrient availability,
319 *Atmos. Chem. Phys.*, 16, 4579–4591, 2016.

320 Carlton, A. G. and Turpin, B. J.: Particle partitioning potential of organic compounds
321 is highest in the Eastern US and driven by anthropogenic water, *Atmos. Chem.*
322 *Phys.*, 13, 10203–10214, 2013.

323 Chang, R. Y.-W., Slowik, J. G., Shantz, N. C., Vlasenko, A., Liggio, J., Sjostedt, S. J.,
324 Leaitch, W. R., and Abbatt, J. P. D.: The hygroscopicity parameter (κ) of
325 ambient organic aerosol at a field site subject to biogenic and anthropogenic
326 influences: relationship to degree of aerosol oxidation, *Atmos. Chem. Phys.*,
327 10, 5047–5064, 2010.

328 Deetz, K., Vogel, H., Haslett, S., Knippertz, P., Coe, H., and Vogel, B.: Aerosol liquid
329 water content in the moist southern West African monsoon layer and its
330 radiative impact, *Atmos. Chem. Phys.*, 18, 14271–14295, 2018.

331 Donahue, N. M., Robinson, A. L., Stanier, C. O., and Pandis, S. N.: Coupled
332 partitioning, dilution, and chemical aging of semivolatile organics, *Environ.*
333 *Sci. Technol.*, 40, 2635–2643, 2006. *Environ: Comprehensive Air Quality*
334 *Model with Extensions Version 4.40. Users Guide. ENVIRON Int. Corp.,*
335 *Novato, CA, <http://www.camx.com>, 2006.*

336 [Fahey, K. and Pandis, S. N.: Optimizing model performance: variable size resolution](#)
337 [in cloud chemistry modeling, *Atmos. Environ.*, 35, 4471–4478, 2001.](#)

Formatted: English (United States)

338 Fountoukis, C. and Nenes, A.: ISORROPIA II: a computationally efficient
339 thermodynamic equilibrium model for K^+ - Ca^{2+} - Mg^{2+} - NH_4^+ - Na^+ - SO_4^{2-} - NO_3^- -
340 Cl^- - H_2O aerosols, *Atmos. Chem. Phys.*, 7, 4639–4659, 2007.

341 Fountoukis, C., Nenes, A., Sullivan, A., Weber, R., Van Reken, T., Fischer, M.,
342 Matías, E., Moya, M., Farmer, D., and Cohen, R. C.: Thermodynamic
343 characterization of Mexico City aerosol during MILAGRO 2006, *Atmos.*
344 *Chem. Phys.*, 9, 2141–2156, 2009.

345 Fountoukis, C., Megaritis, A. G., Skyllakou, K., Charalampidis, P. E.,
346 Denier van der Gon, H. A. C., Crippa, M., Prévôt, A. S. H., Fachinger, F.,
347 Wiedensohler, A., Pilinis, C., and Pandis, S. N.: Simulating the formation of
348 carbonaceous aerosol in a European Megacity (Paris) during the MEGAPOLI
349 summer and winter campaigns, *Atmos. Chem. Phys.*, 16, 3727–3741, 2016.

350 Freney, E. J., Sellegri, K., Canonaco, F., Colomb, A., Borbon, A., Michoud, V.,
351 Doussin, J.-F., Crumeyrolle, S., Amarouche, N., Pichon, J.-M., Bourianne, T.,
352 Gomes, L., Prevot, A. S. H., Beekmann, M., and Schwarzenböeck, A.:
353 Characterizing the impact of urban emissions on regional aerosol particles:
354 airborne measurements during the MEGAPOLI experiment, *Atmos. Chem.*
355 *Phys.*, 14, 1397–1412, 2014.

356 Gopinath, A. K., Raj, S. S., Kommula, S. M., Jose, C., Panda, U., Bishambu, Y.,
357 Ojha, N., Ravikrishna, R., Liu, P., and Gunthe, S. S.: Complex ~~i~~nterplay
358 ~~b~~etween ~~o~~rganic and ~~s~~secondary ~~i~~norganic ~~a~~aerosols ~~w~~with ~~a~~ambient
359 ~~r~~relative ~~h~~umidity ~~i~~mplicates the ~~a~~aerosol ~~l~~iquid ~~w~~water ~~c~~content ~~o~~ver
360 India ~~d~~during ~~w~~wintertime, ~~J~~ournal of Geophysical Research: ~~A~~tmospheres,
361 127, ~~(43)~~, e2021JD036430, 2022.

362 Gunthe, S. S., Liu, P., Panda, U., Raj, S. S., Sharma, A., Derbyshire, E., Reyes-
363 Villegas E., Allan, J., Chen, Y., Wang, X., Song, S., Pöhlker, M. L., Shi, L.,
364 Wang, Y., Kommula, S. M., Liu, T., Ravikrishna, R., McFiggans, G., Mickey,
365 L. J., Martin, S. T., Pöschl, U., Andreae, M. O., and Coe, H.: Enhanced
366 aerosol particle growth sustained by high continental chlorine emission in
367 India., *Nat. Geosci.*, 14, 77–84, 2021.

Field Code Changed

368 Guo, H., Xu, L., Bougiatioti, A., Cerully, K. M., Capps, S. L., Hite Jr., J. R., Carlton,
369 A. G., Lee, S.-H., Bergin, M. H., Ng, N. L., Nenes, A., and Weber, R. J.: Fine-

Field Code Changed

370 particle water and pH in the southeastern United States, *Atmos. Chem. Phys.*
371 15, 5211–5228, 2015.

372 Guo, H., Liu, J., Froyd, K. D., Roberts, J. M., Veres, P. R., Hayes, P. L., Jimenez, J.
373 L., Nenes, A., and Weber, R. J.: Fine particle pH and gas–particle phase
374 partitioning of inorganic species in Pasadena, California, during the 2010
375 CalNex campaign, *Atmos. Chem. Phys.*, 17, 5703–5719, 2017.

376 Guo, H., Li, X., Li, W., Wu, J., Wang, S., and Wei, J.: Climatic modification effects
377 on the association between PM₁ and lung cancer incidence in China, *BMC*
378 *public health*, 21, 880, 2021.

379 Jathar, S.H., Mahmud, A., Barsanti, K.C., Asher, W. E., Pankow, J. F., and Kleeman
380 M. J.: Water uptake by organic aerosol and its influence on gas/particle
381 partitioning of secondary organic aerosol in the United States, *Atmos.*
382 *Environ.*, 129, 142–154, 2016.

383 Jin, X., Wang, Y., Li, Z., Zhang, F., Xu, W., Sun, Y., Fan, X., Chen, G., Wu, H., Ren,
384 J., Wang, Q., and Cribb, M.: Significant contribution of organics to aerosol
385 liquid water content in winter in Beijing, China, *Atmos. Chem. Phys.*, 20,
386 901–914, 2020.

387 Kakavas, S., Pandis, S. N., and Nenes, A.: ISORROPIA-lite: A comprehensive
388 atmospheric aerosol thermodynamics module for Earth System Models, *Tellus*
389 *B*, 74, 1–23, 2022.

390 Karamchandani, P., Vijayaraghavan, K., and Yarwood, G.: Sub-grid scale plume
391 modeling, *Atmosphere*, 2, 389–406, 2011.

392 Karydis, V. A., Tsimpidi, A. P., Fountoukis, C., Nenes, A., Zavala, M., Lei, W.,
393 Molina, L. T., and Pandis, S. N.: Simulating the fine and coarse inorganic
394 particulate matter concentrations in a polluted megacity, *Atmos. Environ.*, 44,
395 608–620, 2010.

396 Kodros, J. K., Papanastasiou, D. K., Paglione, M., Masiol, M., Squizzato, S., Florou,
397 K., Skyllakou, K., Kaltsonoudis, C., Nenes, A., and Pandis, S. N.: Rapid
398 **d**Dark **a**Aging of **b**Biomass **b**Burning as an **o**Overlooked **s**Source of
399 **o**Oxidized **o**Organic **a**Aerosol., *Proc. Natl. Acad. Sci. U.S.A.*, 117,
400 33028–33033, 2020.

401 Koehler, K. A., Kreidenweis, S. M., DeMott, P. J., Petters, M. D., Prenni, A. J., and
402 Carrico, C. M.: Hygroscopicity and cloud droplet activation of mineral dust
403 aerosol, *Geoph. Res. Lett.*, 36, (8), 2009.

404 [Koo, B., Pandis, S. N., and Ansari, A.: Integrated approaches to modeling the organic](#)
405 [and inorganic atmospheric aerosol components, *Atmos. Environ.*, 37, 4757-](#)
406 [4768, 2003.](#)

407 Kostenidou, E., Pathak, R. K., and Pandis, S. N.: An algorithm for the calculation of
408 secondary organic aerosol density combining AMS and SMPS data, *Aerosol*
409 *Sci. Technol.*, 41, ~~(11)~~, 1002–1010, 2007.

410 Kuang, Y., Zhao, C. S., Zhao, G., Tao, J. C., Xu, W., Ma, N., and Bian, Y. X.: A
411 novel method for calculating ambient aerosol liquid water content based on
412 measurements of a humidified nephelometer system, *Atmospheric*
413 *Measurement Techniques*, 11, 2967–2982, 2018.

414 Kuang, Y., Xu, W., Tao, J., Ma, N., Zhao, C., and Shao, M.: A review on laboratory
415 studies and field measurements of atmospheric organic aerosol hygroscopicity
416 and its parameterization based on oxidation levels, *Current Pollution Reports*,
417 10.1007/s40726-020-00164-2, 2020.

418 Li, X., Song, S., Zhou, W., Hao, J., Worsnop, D. R., and Jiang, J.: Interactions
419 between aerosol organic components and liquid water content during haze
420 episodes in Beijing, *Atmos. Chem. Phys.*, 19, 12163–12174, 2019.

421 Li, J., Zhang, H., Ying, Q., Wu, Z., Zhang, Y., Wang, X., Li, X., Sun, Y., Hu, M.,
422 Zhang, Y., and Hu, J.: Impacts of water partitioning and polarity of organic
423 compounds on secondary organic aerosol over eastern China, *Atmos. Chem.*
424 *Phys.*, 20, 7291–7306, 2020.

425 Liao, H. and Seinfeld, J. H.: Global impacts of gas-phase chemistry aerosol
426 interactions on direct radiative forcing by anthropogenic aerosols and ozone, *J.*
427 *Geophys. Res.*, 110, D18208, 2005.

428 Metzger, S., Mihalopoulos, N., and Lelieveld, J.: Importance of mineral cations and
429 organics in gas-aerosol partitioning of reactive nitrogen compounds: case
430 study based on MINOS results., *Atmos. Chem. Phys.*, 6, 2549–2567, 2006.

431 Murphy, B. N. and Pandis, S. N.: Exploring summertime organic aerosol formation in
432 the Eastern United States using a regional-scale budget approach and ambient
433 measurements, *J. Geophys. Res.*, 115, ~~(D24216)~~, 2010.

434 Nenes, A., Pandis, S. N., Weber, R. J., and Russell, A.: Aerosol pH and liquid water
435 content determine when particulate matter is sensitive to ammonia and nitrate
436 availability, *Atmos. Chem. Phys.*, 20, 3249–3258, 2020.

437 Nenes, A., Pandis, S. N., Kanakidou, M., Russell, A. G., Song, S., Vasilakos, P., and
438 Weber, R. J.: Aerosol acidity and liquid water content regulate the dry
439 deposition of inorganic reactive nitrogen, *Atmos. Chem. Phys.*, 21, 6023–
440 6033, 2021.

441 Nguyen, T. K. V., Zhang, Q., Jimenez, J. L., Pike, M., and Carlton, A. G.: Liquid
442 water: ubiquitous contributor to aerosol mass. *Environ. Sci. Tech. Lett.*, 3,
443 257–263, 2016.

444 [Pandis, S. N. and Seinfeld, J. H.: Sensitivity analysis of a chemical mechanism for
445 aqueous-phase atmospheric chemistry, *J. Geophys. Res.*, 94, 1105-1126, 1989.](#)

446 Pandis, S. N., Wexler, A. S., and Seinfeld, J. H.: Secondary organic aerosol formation
447 and transport – II. Predicting the ambient secondary organic aerosol size
448 distribution, *Atmos. Environ.*, 27, 2403–2416, 1993.

449 Petters, M. D., Prenni, A. J., Kreidenweis, S. M., DeMott, P. J., Matsunaga, A., Lim,
450 Y. B., and Ziemann, P. J.: Chemical aging and the hydrophobic-to-hydrophilic
451 conversion of carbonaceous aerosol, *Geophys. Res. Lett.*, 33, L24806, 2006.

452 Petters, M. D. and Kreidenweis, S. M.: A single parameter representation of
453 hygroscopic growth and cloud condensation nucleus activity, *Atmos. Chem.
454 Phys.*, 7, 1961–1971, 2007.

455 [Pilinis, C., Pandis, S. N., and Seinfeld, J. H.: Sensitivity of direct climate forcing by
456 atmospheric aerosols to aerosol size and composition, *Journal of Geophysical
457 Research*, 100\(D9\), 18739, 1995.](#)

458 Pye, H. O. T., Nenes, A., Alexander, B., Ault, A. P., Barth, M. C., Clegg, S. L.,
459 Collett Jr, J. L., Fahey, K. M., Hennigan, C. J., Herrmann, H., Kanakidou, M.,
460 Kelly, J. T., Ku, I.-T., McNeill, V. F., Riemer, N., Schaefer, T., Shi, G.,
461 Tilgner, A., Walker, J. T., Wang, T., Weber, R., Xing, J., Zaveri, R. A., and
462 Zuend, A.: The acidity of atmospheric particles and clouds, *Atmos. Chem.
463 Phys.*, 20, 4809–4888, 2020.

464 Seinfeld, J. H. and Pandis, S. N.: *Atmospheric chemistry and physics: From air
465 pollution to climate change*, Wiley: New York, 2006.

466 Skyllakou, K., Murphy, B. N., Megaritis, A. G., Fountoukis, C., and Pandis, S. N.:
467 Contributions of local and regional sources to fine PM in the megacity of
468 Paris, *Atmos. Chem. Phys.*, 14, 2343–2352, 2014.

469 Skyllakou, K., Rivera, P. G., Dinkelacker, B., Karnezi, E., Kioutsioukis, I.,
470 Hernandez, C., Adams, P. J., and Pandis, S. N.: Changes in

Formatted: English (United States)

471 PM_{2.5} concentrations and their sources in the US from 1990 to 2010, *Atmos.*
472 *Chem. Phys.*, 21, 17115–17132, 2021.

473 Song, S., Gao, M., Xu, W., Shao, J., Shi, G., Wang, S., Wang, Y., Sun, Y., and
474 McElroy, M. B.: Fine-particle pH for Beijing winter haze as inferred from
475 different thermodynamic equilibrium models, *Atmos. Chem. Phys.*, 18, 7423–
476 7438, 2018.

477 [Strader, R., Gurciullo, C., Pandis, S. N., Kumar, N., and Lurmann, F. W.:](#)
478 [Development of gas-phase chemistry, secondary organic aerosol, and aqueous-](#)
479 [phase chemistry modules for PM modeling, Final report for CRC Project A21-](#)
480 [1 prepared for the Coordinating Research Council, Atlanta, GA by Sonoma](#)
481 [Technology, Inc., Petaluma, CA, 1998.](#)

482 Sun, X., Ivey, C. E., Baker, K. R., Nenes, A., Lareau, N. P., and Holmes, H. A.:
483 Confronting Uncertainties of Simulated Air Pollution Concentrations during
484 Persistent Cold Air Pool Events in the Salt Lake Valley, Utah., *Environ. Sci.*
485 *Technol.*, 55, 15072–15081, 2021.

486 Tsimpidi, A. P., Karydis, V. A., Zavala, M., Lei, W., Molina, L., Ulbrich, I. M.,
487 Jimenez, J. L., and Pandis, S. N.: Evaluation of the volatility basis-set
488 approach for the simulation of organic aerosol formation in the Mexico City
489 metropolitan area, *Atmos. Chem. Phys.*, 10, 525–546, 2010.

490 Turpin, B. J. and Lim, H. J.: Species Contributions to PM_{2.5} Mass Concentrations:
491 Revisiting Common Assumptions for Estimating Organic Mass, *Aerosol Sci.*
492 *Technol.*, 35, (1), 602–610, 2001.

493 Wu, Z., Wang, Y., Tan, T., Zhu, Y., Li, M., Shang, D., Wang, H., Lu, K., Guo, S.,
494 Zeng, L., and Zhang, Y.: Aerosol liquid water driven by anthropogenic
495 inorganic salts: Implying its key role in haze formation over the North China
496 Plain, *Environmental Science & Technology Letters*,
497 10.1021/acs.estlett.8b00021, 2018.

498 Xing, J., Pleim, J., Mathur, R., Pouliot, G., Hogrefe, C., Gan, C.-M., and Wei, C.:
499 Historical gaseous and primary aerosol emissions in the United States from
500 1990 to 2010, *Atmos. Chem. Phys.*, 13, 7531–7549, 2013.

501 Yarwood, G., Rao, S., Yocke, M., and Whitten, G. Z.: Updates to the Carbon Bond
502 Chemical Mechanism: CB05, Research Triangle Park, [https://camx-
wp.azurewebsites.net/Files/CB05_Final_Report_120805.pdf](https://camx-
503 wp.azurewebsites.net/Files/CB05_Final_Report_120805.pdf), 2005.

504 Zakoura, M. and Pandis, S. N.: Improving fine aerosol nitrate predictions using a
505 Plume-in-Grid modeling approach, *Atmos. Environ.*, 215, 116887, 2019.

506 Zhang, Q. J., Beekmann, M., Drewnick, F., Freutel, F., Schneider, J., Crippa, M.,
507 Prevot, A. S. H., Baltensperger, U., Poulain, L., Wiedensohler, A., Sciare, J.,
508 Gros, V., Borbon, A., Colomb, A., Michoud, V., Doussin, J.-F., Denier van
509 der Gon, H. A. C., Haefelin, M., Dupont, J.-C., Siour, G., Petetin, H.,
510 Bessagnet, B., Pandis, S. N., Hodzic, A., Sanchez, O., Honoré, C., and
511 Perrussel, O.: Formation of organic aerosol in the Paris region during the
512 MEGAPOLI summer campaign: evaluation of the volatility basis-set approach
513 within the CHIMERE model, *Atmos. Chem. Phys.*, 13, 5767–5790, 2013.

514

515

516

517

518

519

520

521

522

523

524

525

526

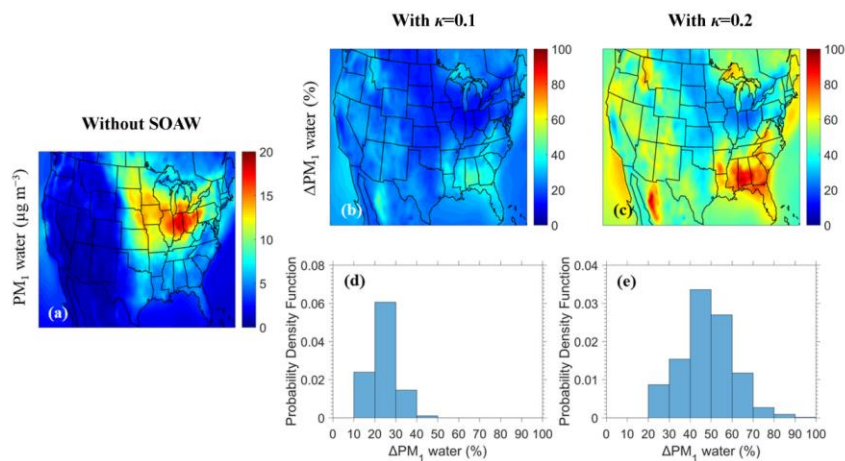
527

528

529

530

531



532

533

534 **Figure 1.** Maps of: (a) annual average PM₁ water ground-level concentrations
535 neglecting SOAW, (b) annual average fractional increase of PM₁ water when SOAW
536 is present in the simulations with $\kappa=0.1$ and, (c) with $\kappa=0.2$ during 2010. The
537 probability density as a function of fractional increase in the annual PM₁ water
538 concentrations due to SOAW when: (d) $\kappa=0.1$ and (e) $\kappa=0.2$ is shown.

539

540

541

542

543

544

545

546

547

548

549

550

551

552

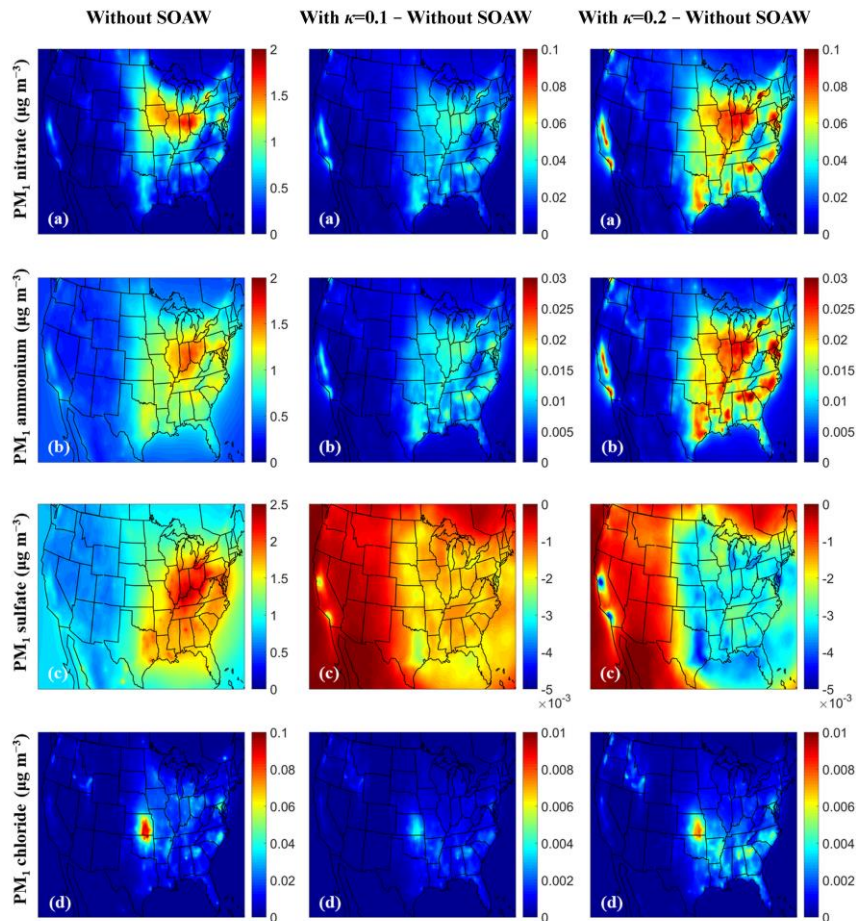
553

554

555

556

557



558

559

560 **Figure 2.** Annual average ground-level concentrations (in $\mu\text{g m}^{-3}$) of PM₁: (a) nitrate,
 561 (b) ammonium, (c) sulfate, and (d) chloride neglecting SOAW and the annual
 562 concentration changes when SOAW is present in the simulations with $\kappa=0.1$ and
 563 $\kappa=0.2$. A positive change corresponds to an increase. A negative change corresponds
 564 to a decrease.

565

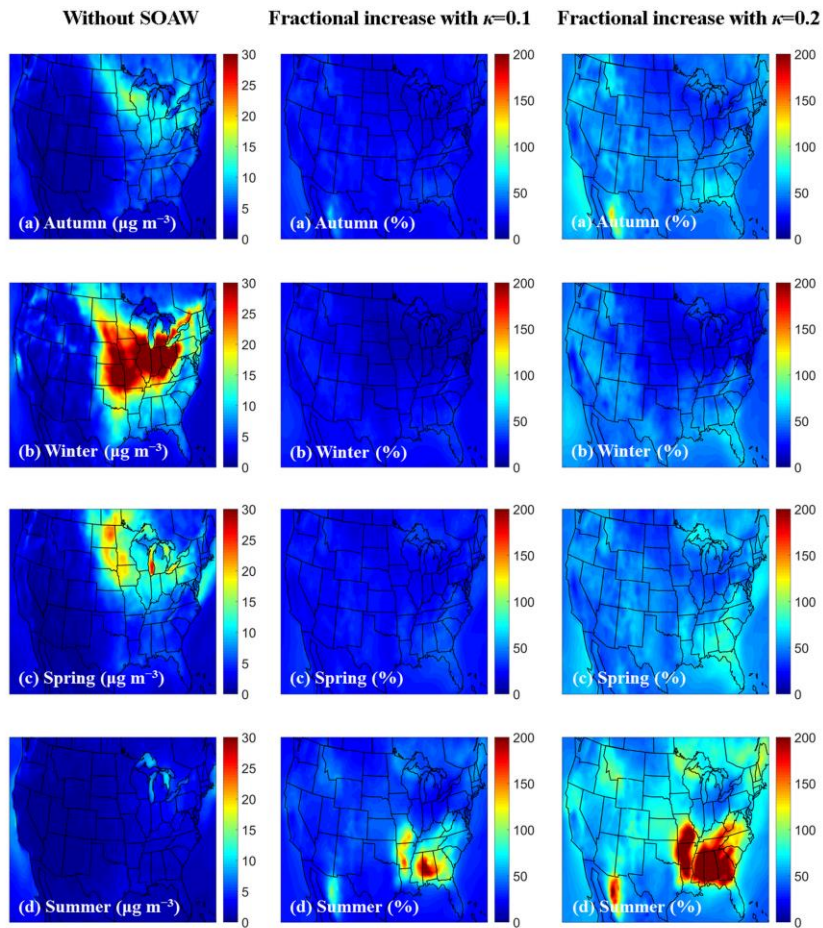
566

567

568

569

570



571

572

573 **Figure 3.** Average ground-level concentrations of PM₁ water neglecting SOAW (in
 574 $\mu\text{g m}^{-3}$) and the fractional increase when SOAW is present in the simulations with
 575 $\kappa=0.1$ and $\kappa=0.2$ during: (a) autumn (SON), (b) winter (DJF), (c) spring (MAM), and
 576 (d) summer (JJA) of 2010.

577

578

579

580

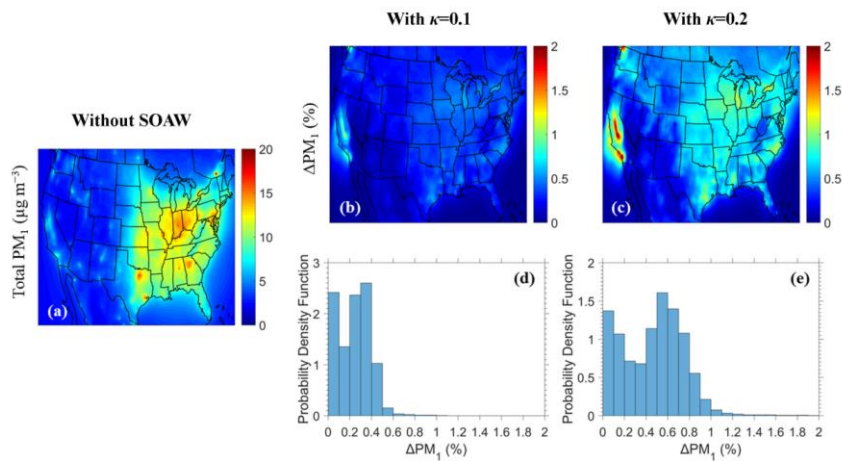
581

582

583

584

585
586

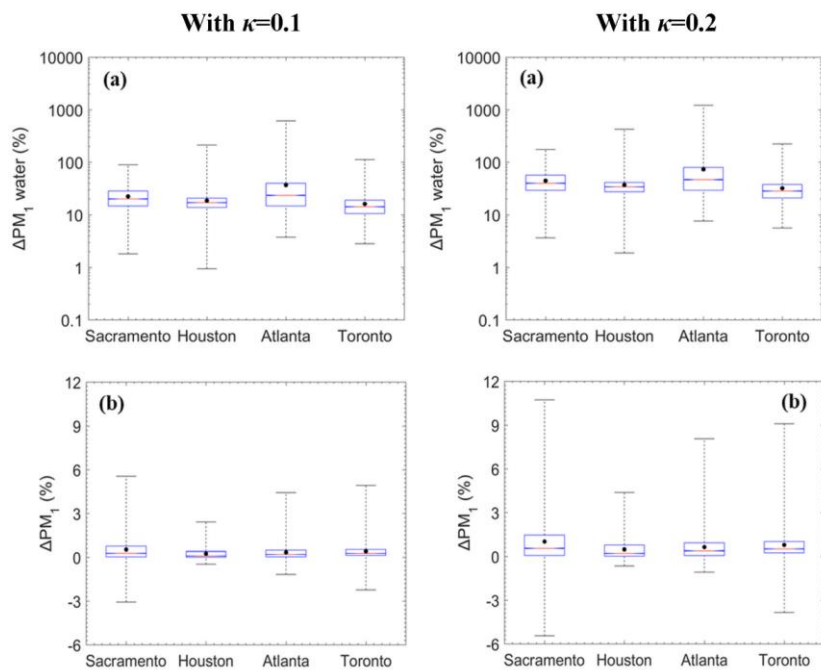


587
588

589 **Figure 4.** Maps of: (a) annual average total dry PM₁ ground-level concentrations
590 neglecting SOAW, (b) annual average fractional increase of total dry PM₁ when
591 SOAW is present in the simulations with $\kappa=0.1$ and, (c) with $\kappa=0.2$ during 2010. The
592 probability density as a function of fractional increase in the annual total dry PM₁
593 concentrations due to SOAW when: (d) $\kappa=0.1$ and (e) $\kappa=0.2$ is shown.

594
595
596
597
598
599
600
601
602
603
604
605
606
607
608
609
610
611
612
613
614
615
616
617

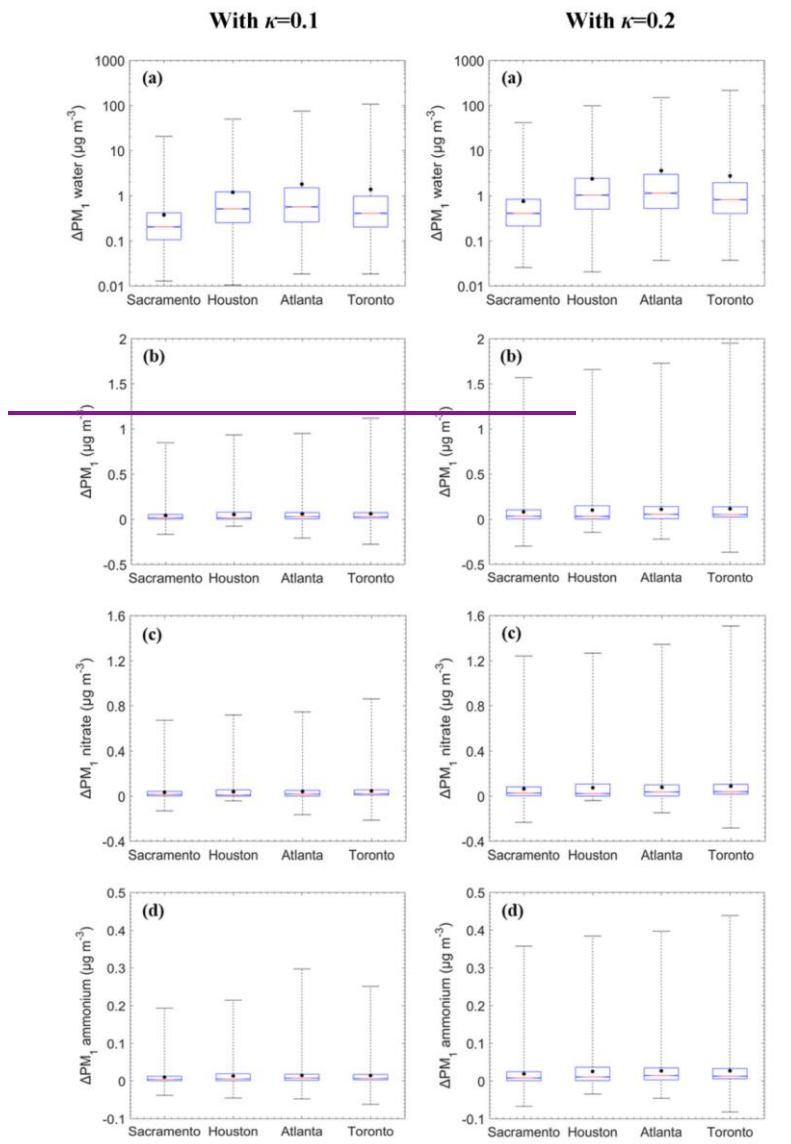
618
619



620
621

622 **Figure 5.** Box plots for fractional change in the hourly: (a) PM_1 water and (b) total
623 dry PM_1 due to SOAW when $\kappa=0.1$ and $\kappa=0.2$ for Sacramento, California; Houston,
624 Texas; Atlanta, Georgia; and Toronto, Canada during 2010. The red line represents
625 the median, the black dot is the mean value, the upper box line is the upper quartile
626 (75%) and the lower box line is the lower quartile (25%) of the distribution. A
627 negative change corresponds to a decrease.

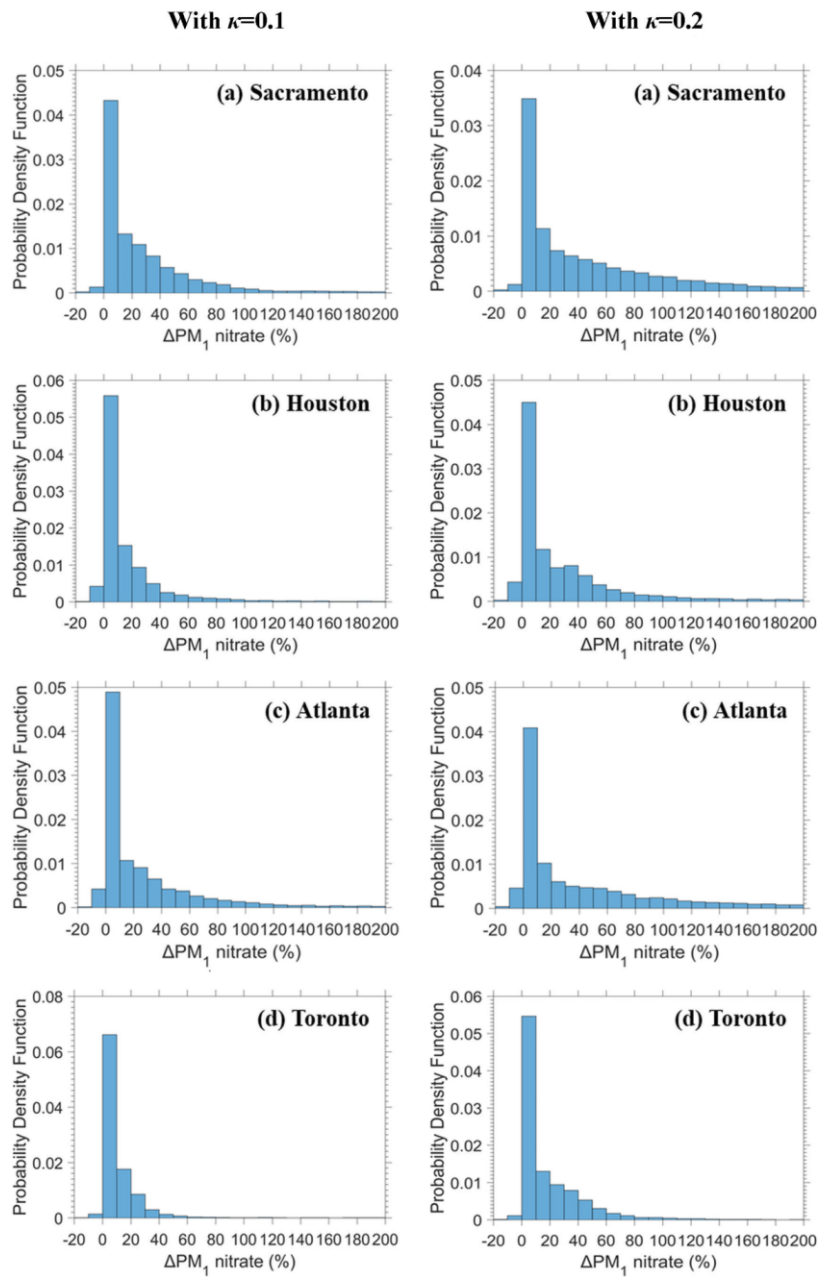
628
629
630
631
632
633
634
635
636
637
638
639
640
641
642



643
644
645
646
647
648
649
650
651
652

Figure 6. Box plots for concentration changes in the hourly PM₁: (a) water, (b) total dry, (c) nitrate, and (d) ammonium due to SOAW when $\kappa=0.1$ and $\kappa=0.2$ for Sacramento, California; Houston, Texas; Atlanta, Georgia; and Toronto, Canada during 2010. The red line represents the median, the black dot is the mean value, the upper box line is the upper quartile (75%) and the lower box line is the lower quartile (25%) of the distribution. A negative change corresponds to a decrease. Water is in log scale to show clearly both the relatively small average and the large range of high values.

Commented [Σ11]: Reviewer 4 Comment 3



653
654

655 **Figure 67.** The probability density as a function of fractional increase in the hourly
656 PM_1 nitrate due to SOAW when $\kappa=0.1$ and $\kappa=0.2$ for: (a) Sacramento, California; (b)
657 Houston, Texas; (c) Atlanta, Georgia; and (d) Toronto, Canada during 2010.